Proceedings of the ASME 2020
International Mechanical Engineering Congress and Exposition
IMECE2020
November 15-19, 2020, Portland, OR, USA

IMECE2020-24400

INVESTIGATION OF ADDITIVE MANUFACTURED GRCOP-42 ALLOY DEVELOPED BY DIRECTED ENERGY DEPOSITION METHODS

Scott Landes[1], Trupti Suresh[1], Anamika Prasad[1], Todd Letcher[1]
[1]Mechanical Engineering Department,
South Dakota State University,
Brookings, SD

Paul Gradl[2], David Ellis[3]
[2]Senior Combustion Devices Engineer,
NASA Marshall Space Flight Center, Huntsville, AL
[3]Material Research Engineer,
NASA Glenn Research Center, Cleveland, OH

ABSTRACT

GRCop is an alloy family constructed of copper, chromium, and niobium and was developed by NASA for high heat flux applications. GRCop-alloys were specifically formulated for the requirements in channel-cooled main combustion chambers allowing for repeat use in high heat flux environments. GRCop-84 was evolved using additive manufacturing techniques under a NASA development program. To further increase thermal conductivity while maintaining material strength characteristics, the percentage of alloying elements were cut in half and GRCop-42 was developed. In recent years, NASA has successfully additively manufactured GRCop-42 using a laser Powder Bed Fusion (L-PBF) process. The L-PBF process was found to produce material properties comparable to traditionally extruded GRCop-42. Benefits of this process include fabrication of intricate internal cooling channels as well as a decrease in manufacturing time. However, there are some large disadvantages in using this process. The nature of the powder bed process imposes a strict volume constraint as well as an excessive amount of material inventory required. A Directed Energy Deposition (DED) process addresses these limitations while also speeding up the manufacturing process. With little data on how DED performs with GRCop-42, an investigation into the mechanical properties was conducted. More specifically, Blown Powder Directed Energy Deposition (BPD), was used to compare material properties to that of the L-PBF manufactured GRCop-42. The DED manufactured material was found to have less than 0.1% porosity. Tensile tests concluded that the DED manufactured GRCop-42 had lower tensile strengths at room temperature. The results point towards a process capable of producing fully dense parts capable of meeting mechanical strength requirements with some possible refinement of printing parameters.

Keywords: Additive Manufacturing, Blown Powder Directed Energy Deposition, GRCop-42, BP-DED, BPD

1. INTRODUCTION

GRCop is an alloy family in which copper is alloyed with chromium and niobium. GRCop was designed for high heat flux applications such as regeneratively-cooled main combustion chambers (MCC). These chambers consist of internal coolant channels and manifolds in which liquid propellent flows and is used as a coolant to dissipate heat from the combustion chamber prior to being supplied as fuel in the injector. Figure 1 shows a

FIGURE 1: CROSS SECTIONAL VIEW OF A CHANNEL-COOLED MCC

[1*] Contact Corresponding author: Todd.Letcher@sdstate.edu

sample cross-sectional view perpendicular to the longitudinal axis of a simplified regeneratively-cooled MCC. Similar design and fabrication techniques are used for channel wall nozzles, although many use a lower conductivity and higher strength to weight material to optimize the engine system. To reduce manufacturing costs, NASA has been evaluating several fabrication approaches for channel cooled chambers and nozzles [2].

Within the past years, NASA's Marshall Space Flight Center (MSFC) and Glenn Research Center (GRC) have led the way in exploring the use of additively manufacturing (AM) for spaceflight applications. AM is a process by which material is deposited layer by layer as opposed to traditional forming and machining methods. Specifically, research has been conducted on the performance of AM GRCop-42 using a Laser Powder Bed Fusion (L-PBF) technique [3]. However, L-PBF has its drawbacks in that it requires an excess of powder for each print and the powder bed puts a strict volume constraint on the scalability [4]. A directed energy deposition (DED) AM process has potential to improve upon both of those issues seen in L-PBF. Blown powder directed energy deposition (BPD), a DED process, involves injecting a powder into the path of a high intensity energy source such as a laser. An illustration of this process is shown in Figure 2. DED would allow for the process to be far more scalable, for the main limiting factor is the gantry (or robotic arm) system as opposed to the powder bed volume. Also, the quantity of material required for manufacturing would be significantly reduced since it only requires local deposition.

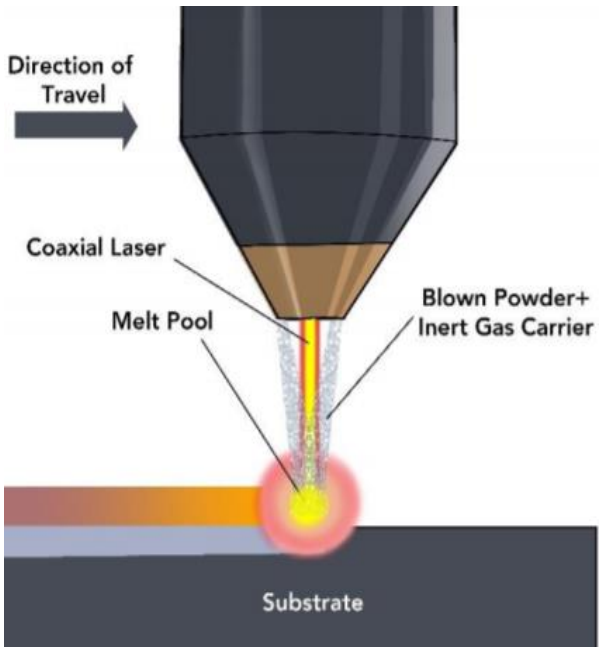

FIGURE 2: DEPICTION OF BLOWN POWDER DED PROCESS [9]

This study aims to investigate DED manufactured GRCop-42 and compare it to the results reported using L-PBF as well as conventional manufacturing methods. Specifically, porosity and tensile strength were investigated and compared. Collecting quantifiable data on the DED manufactured GRCop-42 will yield the research in determining the feasibility and effectiveness of applying this process towards reducing costs of manufacturing for applications such as regeneratively-cooled channel wall combustion chambers.

2. LITERATURE REVIEW

2.1 GRCop Alloy Family

GRCop is a copper-based alloy that was developed at NASA's GRC. The alloy is a dispersion strengthened material. due to the presence of Cr_2Nb intermetallic compound which improves strength and retains microstructure and strength at elevated temperatures [1]. The Cr_2Nb particles make producing this material more difficult because conventional casting methods cannot be used since the Cr_2Nb particles grow to undesirable sizes during the cooling processes. The alloy must be produced using rapid solidification processes such as gas atomization to ensure small Cr_2Nb particles. The powder produced can yield powder size distribution for both the L-PBF and BPD processes, and have a mean of 40um [1]. The powder was traditionally used to fabricate components using conventional fabrication techniques such as extruding or hot isostatic pressing (HIP).

GRCop-84 was the first of the GRCop family. It was specifically designed for the environments seen in regeneratively-cooled combustion chambers for high duty cycle (repeat use). While GRCop-84 proved to provide excellent strength and manufacturability [5], a further increase in thermal conductivity was desired to further enhance heat transfer to help reduce wall temperatures. To increase thermal conductivity while maintaining material strength characteristics, the percentage of alloying elements were cut in half and was therefore designated GRCop-42 [6]. It was found that much of the strength of GRCop-84 was retained at high temperatures in which are normal operating conditions of an MCC liner. Specifically, at temperatures greater than 400 °C, the ultimate tensile strength (UTS) of GRCop-42 was found to nearly be the same as GRCop-84, while both have continued use temperatures exceeding 750 °C [7]. A slight decrease in low-cycle-fatigue life (LCF) was seen when compared to GRCop-84. However, the LCF life of GRCop-42 was still very comparable to NASA's similar high heat flux alloy NARloy-Z (Cu-3%Ag-0.5%Zr) [6] which is used as the MCC liner in the space shuttle main engine (RS-25) [8].

2.2 Additive Manufacturing of GRCop

Starting in 2014, NASA started on a development of producing GRCop-84 using L-PBF. Copper has challenges associated with AM due to its high thermal conductivity and reflectiveness. However, GRCop-84 was proved to be successfully manufactured using L-PBF which led to several component fabrication trials and successful hot-fire tests in 2016 and 2017 at MSFC [9]. This led to the more defined development

of GRCop-42 since a need for a higher thermally conductive material was foreseen. Along with the process development, the powder supply chains had to be evolved to meet requirements for minimal oxidation and trace elements and meet the distributions required for additive manufacturing.

In K.G. Cooper's et al. "Three-Dimensional Printing GRCop-42" an AM process for producing GRCop-42 was developed [3]. Based on the previous AM work with GRCop-84, a Concept Laser M2 was used to produce the L-PBF AM samples. A matrix of data was collected where laser scan speed and power were varied while overall porosity and average pore size were recorded. This allowed for optimum printing parameters of GRCop-42 to be determined.

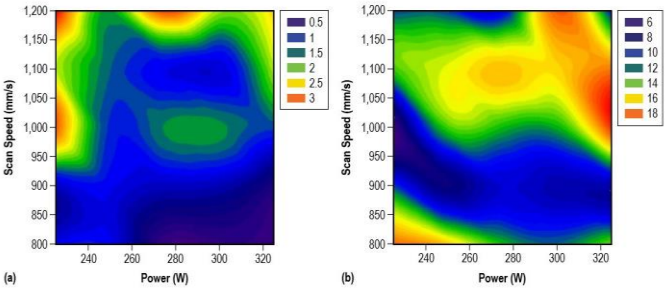

FIGURE 3: POROSITY RESULTS OF PBF MANUFACTURED GRCOP-42 [3]

The optimum printing parameters were then used for producing specimens for room temperature tensile tests. Twenty-five specimens were printed and then post-processed through a HIPing cycle typically used for the GRCop-84 L-PBF material. The printed specimens were machined to specification for ASTM E8-style round specimens [10]. Based on tests on 20 samples, the ultimate tensile strength (UTS) was obtained between 339 MPa to 356 MPa and elongations >20%. The study showed that GRCop-42 alloy component could be additively manufactured with properties comparable and even superior to its traditionally manufactured predecessors [3].

From the previous works described, it was concluded that GRCop-84 and GRCop-42 were capable of being additively manufactured using PBF methods. To further evaluate the capability of AM GRCop, hot-fire tests were conducted. In 2019, a "bimetallic hybrid additively manufactured combustion chamber" was manufactured and successfully hot-fired using GRCop-84 for the MCC liner [9]. The liner was manufactured using a L-PBF process, while an Inconel 625 structural jacket was cladded to the liner using a hybrid blown powder DED (BPD) process. The hybrid AM approach uses the BPD process to deposit material onto the L-PBF liner with an integral machining capability in a single setup. Similarly, AM GRCop-42 using L-PBF has completed a significant number of hot-fire tests using various configurations including a "slip-jacket channel-cooled chamber configuration" [7].

These results could be directly compared to the performance of a L-PBF additively manufactured GRCop-84 chamber that was tested in the same way a year prior [11]. Vital information was gathered from these tests such that the performance of AM combustion chamber can be benchmarked against traditionally manufactured ones. The data demonstrated that L-PBF liners were of high performance and could be produced at >50% schedule reductions and lower costs compared to those traditionally manufactured. The technology is now being evaluated by several commercial space companies.

Both GRCop alloys have been successfully manufactured using AM. However, it must be noted that GRCop-42 has \ benefits over GRCop-84 in terms of its higher thermal conductivity with similar strength, which makes it more desirable to produce MCC liners. Additionally, the build speeds have proven to be 20% faster for the GRCop-42 over the GRCop-84, which helps further reduce costs [3]. Lastly, some powder vendors commented that the GRCop-42 was easier to produce over the GRCop-84, so a more readily available powder supply chain is available at a lower cost. GRCop-42 is the primary material being explored for NASA and many commercial service vendors making it available across industry.

3. MATERIALS AND METHODS

3.1 Sample Preparation

Two batches of the GRCop-42 material were additively manufactured using BPD with a 45-105um powder size. The second batch went through a Hot Isostatic Pressing (HIP) process while the first batch was provided as-built. The material was built up on a thick substrate, which is required for BPD. Figure

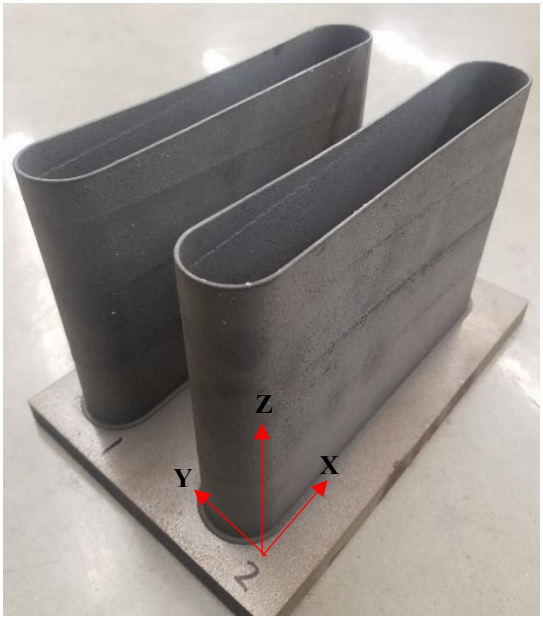

FIGURE 4: EXAMPLE OF MATERIAL RECEIVED PRIOR TO MATERIAL PROCESSING (HIP'D BATCH)

4 displays the HIP'd material. A band saw was used to cut the part down into sheets. All tested samples were then cut from these sheets. Tensile specimens were cut by a water jet. The

specimens were cut from the sheets so nearly half of them were oriented in such that the print layers were in the longitudinal direction (parallel to x-axis). The rest of the specimens were oriented such that the print layers were in the lateral direction (parallel to z-axis). Tensile specimens were sized in accordance

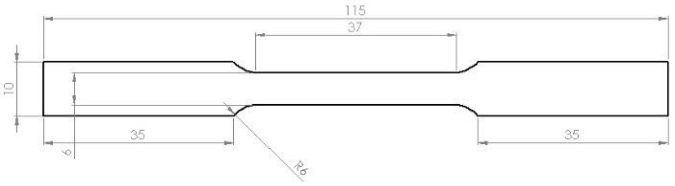

FIGURE 5: TENSILE TEST SPECIMEN SIZING SPECIFICATION

to ASTM E8 [10] and the dimensions are shown in Figure 5. All the tensile testing was conducted with the second batch of material only in the HIP'd condition, as this is how it would be used in an actual application. In addition, eight samples of roughly 7mm by 7mm were cut from each set of material. These samples were then used for porosity measurements.

3.2 Porosity Measurement

Porosity measurements were determined using a microscopy-based method. Porosity samples were first mounted in Buehler's EpoxiCure 2 (thermosetting resin) such that the printed layers were visible. The mounted samples were then ground down until the internal surface of the material was fully exposed. To start, a silicon carbide paper of 400 grit was used until a uniform surface finish was achieved. This process was then repeated down to 1200 grit. Next, the samples were polished using a diamond suspension starting at 6 μm and working down to 0.25 μm. The samples were then finished with a colloidal silica suspension of 0.05 μm. Immediately after polishing, the samples were placed in an ultrasonic cleaner of ethanol for 15 min. This resulted in a mirror like finish that was free of any material defects imposed by the polishing process. Next, a Keyence VK-9710 microscope was used to take a stitched image of the entire sample at 1200x magnification as seen in Figure 6. The image was then post-processed using ImageJ software [12].

ImageJ is an open source image processing software and was used for quantifying all porosity values. First, the image was changed to an 8-bit binary (greyscale) image. This applies a single greyscale intensity value from 0 to 256 to each pixel throughout the image where a pixel of intensity value 0 is black and a pixel of 256 is white. Due to the large contrast that the pores and mounting material have with the surface finish of the copper alloy, a distribution of higher intensity values and lower intensity values are seen. A threshold can be applied to these distributions to create a two color (black and white) image. ImageJ's default thresholding model was used for all porosity measurements. The resulting image is shown in Figure 7. A particle analysis within the software was then applied to the sample surface to calculate for a porosity. Porosity is simply the void volume within the material divided by the total volume. In this case, a 2d section of the volume is visible and area is used instead of volume. This porosity calculation is shown in equation 1. Where the black pixels in the images represents the area of voids.

$$Porosity\ (\%) = \frac{Volume\ of\ Voids}{Total\ Volume} * 100 \qquad (1)$$

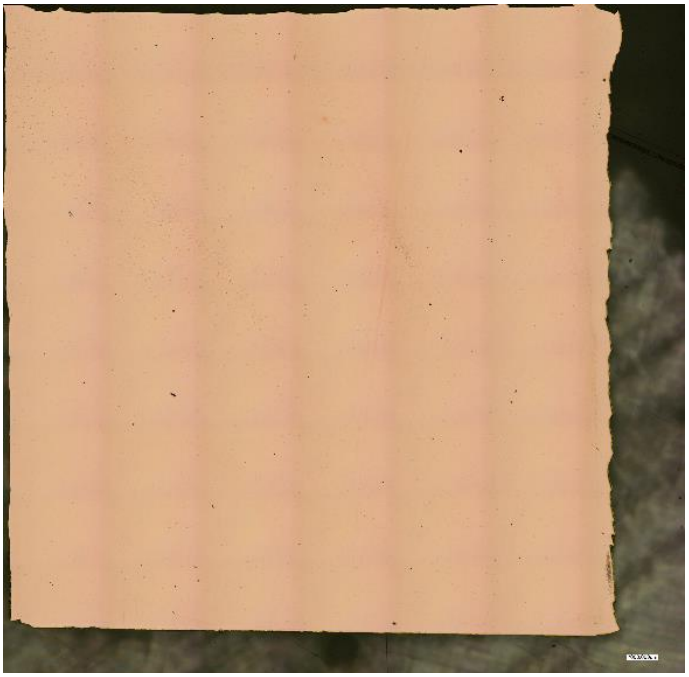

FIGURE 6: EXAMPLE OF INITIAL STITCHED IMAGE USED IN POROSITY MEASUREMENTS

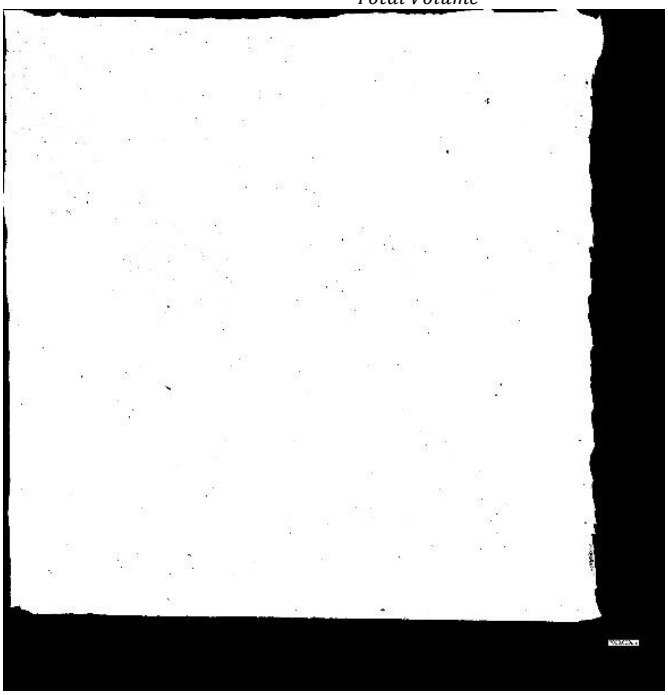

FIGURE 7: EXAMPLE OF FINAL IMAGE USED IN POROSITY MEASUREMENTS

3.3 Tensile Testing

All tensile tests were conducted on an MTS 858 universal testing machine. The tests were displacement controlled at 0.375 mm/min. A total of 10 tensile tests were conducted at various temperatures. Prior to starting each test, the specimen was lightly sanded to smooth the surface to reduce the effects that the layers and surface roughness would cause on cross-sectional area measurements. Width and thickness measurements were taken at five different locations along the gage length of each specimen using a caliper. Because the sample changed thickness (slightly) from top to bottom, the location of failure of the tensile test determined the original measurements to calculate cross sectional area for that sample to calculate stresses.

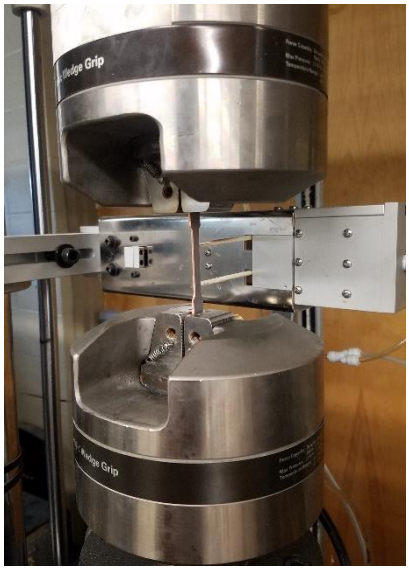

FIGURE 8: TENSILE TESTING SETUP

The ultimate tensile strength and elastic modulus was then calculated using both the original average cross-sectional area as well as the original cross-sectional area at location of failure. Due to the high ductility of the material, the extensometer had to be removed after an extension of approximately 2.5mm (0.11 mm/mm). To determine the maximum strain, an approximated strain was calculated.

4. RESULTS AND DISCUSSION

4.1 Porosity Results

Measurements for the first batch (un-HIP'd) of material of GRCop-42 is shown in Table 1, while Table 2 depicts results from the second batch of material. Porosity values were found to be very low, resulting in near fully dense GRCop-42. Porosity was found to be lower than originally published values of GRCop-42 L-PBF, but show equivalent density to current development with L-PBF samples. However, it must be noted that due to the geometry of the part, the porosity results in this study are representative of the center of the laser path and vertical layering as opposed to part infill or horizontal layering. The porosity found in both the HIP'd and un-HIP'd material was found to be similar in porosity within the tolerances of error. The mean pore diameter was found to stay relatively consistent throughout all samples and was comparable to the PBF results, which ranged from 6-18 μm [3] where the BPD ranged from 5-13 μm.

TABLE 1: POROSITY MEASUREMENTS FROM FIRST BATCH OF MATERIAL (NOT HIP'D)

Sample #	Porosity (%)	Mean Area (μm^2)	Standard deviation (μm^2)	Maximum (μm^2)	Mean Pore Diameter (μm)
1	0.011	23.953	52.504	545.816	5.522
2	0.013	31.634	115.222	1143.331	6.346
3	0.009	136.785	192.160	707.255	13.197
4	0.026	15.918	21.028	261.377	4.502
5	0.015	23.864	60.825	738.005	5.512
6	0.034	33.531	235.992	4873.907	6.534
7	0.031	43.121	256.449	4566.405	7.410
8	0.034	30.515	76.639	907.131	6.233
Average	0.022				

TABLE 2: POROSITY MEASUREMENTS FROM SECOND BATCH OF MATERIAL (HIP'D)

Sample #	Porosity (%)	Mean Area (μm^2)	Standard deviation (μm^2)	Maximum (μm^2)	Mean Pore Diameter (μm)
1	0.087	22.028	45.747	661.087	5.296
2	0.040	27.982	68.099	745.644	5.969
3	0.061	30.252	77.713	1498.975	6.206
4	0.056	31.071	83.708	1598.907	6.290
5	0.047	47.440	85.723	1099.249	7.772
6	0.056	31.992	77.745	1168.432	6.382
7	0.045	38.656	112.960	1591.220	7.016
8	0.036	33.703	94.386	1698.839	6.551
Average	0.054				

4.2 Tensile Results

An example of resultant stress-strain curves are shown below. Specifically, for the lateral specimens at room temperature.

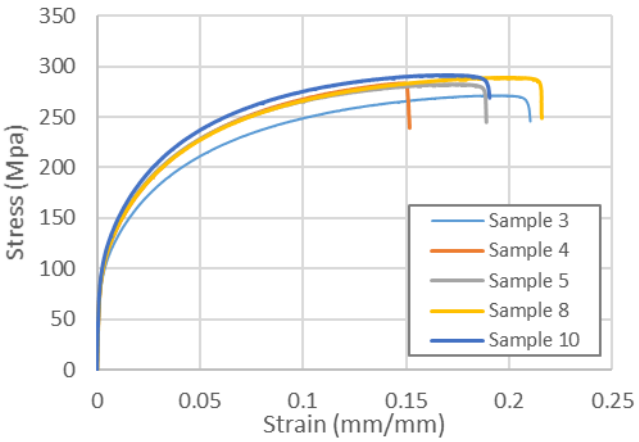

FIGURE 9: LATERAL SPECIMEN STRESS/STRAIN CURVES AT ROOM TEMPERATURE

Ultimate tensile strength, elastic modulus, and maximum strain from the tensile tests of the HIP'd DED GRCop-42 conducted at room temperature are shown in Table 3 and Table 4. Where the first table displays the longitudinal specimens and the second displays the lateral specimen data. It is seen that the longitudinal orientation had a higher average ultimate tensile strength of 297 MPa when compared to the lateral orientation's ultimate tensile strength of 284 MPa. This is a percent difference of 4.6 percent.

The first two specimens tested had faulty extensometer readings. Therefore, the modulus and maximum strain values were unable to be calculated for those specimens. The ultimate tensile strength is clearly seen to have a larger value when the original cross-sectional area at the failure location is used when compared to an average cross-sectional area. However, it does look to increase the standard deviation of the test results as well. As expected, all the failures on the lateral specimens occurred between the print layers.

TABLE 3: LONGITUDINAL ORIENTATION SPECIMEN TENSILE TEST DATA (HIP'D)

Specimen	UTS (MPa)		E (GPa)		Max Strain (mm/mm)
	@ Average Area (mm^2)	@ Failure Area (mm^2)	@ Average Area (mm^2)	@ Failure Area (mm^2)	
01	289.48	294.90	N/A	N/A	N/A
02	304.41	306.39	N/A	N/A	N/A
06	282.91	297.26	116.46	122.36	0.198
07	302.38	306.43	120.55	122.17	0.261
09	305.95	329.70	126.20	136.00	0.323
AVG	297.03	306.94	121.07	126.84	0.260
STD DEV	10.23	13.76	4.89	7.93	0.063

TABLE 4: LATERAL ORIENTATION SPECIMEN TENSILE TEST DATA (HIP'D)

FIGURE 10: TENSILE SAMPLES AFTER TESTING

Specimen	UTS (MPa)		E (GPa)		Max Strain (mm/mm)
	@ Average Area (mm^2)	@ Failure Area (mm^2)	@ Average Area (mm^2)	@ Failure Area (mm^2)	
03	271.42	282.065	107.63	111.85	0.204
04	283.40	298.79	120.09	126.61	0.149
05	282.43	299.42	130.56	138.41	0.188
08	289.18	303.04	154.1	161.48	0.219
10	291.62	301.04	137.51	141.95	0.194
AVG	283.61	296.87	129.98	136.06	0.191
STD DEV	7.83	8.44	17.58	18.45	0.0261

5. CONCLUSION

The porosity results of the BPD manufactured GRCop-42 was found to have some of the lowest porosity values when compared to the published L-PBF manufactured GRCop-42 porosity values [3]. Porosity values of less than 0.1% were found in all the BPD GRCop-42 samples. The jetted powder could reduce on voids that would otherwise be encapsulated by the material in a stagnant material bed used in the PBF process. The BPD was found to be capable of producing near fully dense parts. However, it is recommended that more porosity measurements

are taken on specimens created with horizontal layering to ensure that there is no large variation in porosity when evaluating a different plane of interest. Tensile testing showed that longitudinal orientation specimens had a higher ultimate tensile strength when compared with the lateral specimens. This could be affected by the more pronounced variation in thickness due to the layering effects of the manufacturing process. These layering effects create stress concentrators that result in the lateral specimens failing sooner. The BPD manufactured GRCop-42 was found to have and an average ultimate tensile strength of 290 MPa which has a percent difference of 20% when compared to the L-PBF manufactured GRCop-42 reported ultimate tensile strength of 355 MPa [7] at room temperature.

REFERENCES

[1] D. L. Ellis, "GRCop-84: A High-Temperature Copper Alloy for High-Heat-Flux Applications," NASA, 2005.

[2] P. R. Gradl and C. S. Protz, "Technology advancements for channel wall nozzle manufacturing in liquid rocket engines," *Acta Astronautica,* vol. 174, pp. 148-158, 2020.

[3] K. G. Cooper, J. L. Lydon, M. D. LeCorre, Z. C. Jones, D. S. Scannapieco, D. L. Ellis and B. A. Lerch, "Three-Dimensional Printing GRCop-42," NASA, 2018.

[4] I. Gibson, D. Rosen and B. Stucker, Directed Energy Deposition Processes. In: Additive Manufacturing Technologies., New York: Springer, 2015.

[5] W. Loewenthal and D. Ellis, "Fabrication of GRCop-84 Rocket Thrust Chambers," in *Materials Science and Technology 2005 Conference and Exhibition*, Pittsburgh, 2006.

[6] D. L. Ellis, "Conductivity of GRCop-42 Alloy Enhanced," NASA, 2004.

[7] P. R. Gradl, C. Protz, K. Cooper, C. Garcia, D. Ellis and L. Evans, "GRCop-42 Development and Hot-fire Testing Using Additive Manufacturing Powder Bed Fusion for Channel Cooled Combustion Chambers," in *55th AIAA/SAE/ASEE Joint Propulsion Conference*, Indianapolis, 2019.

[8] B. N. Bhat, S. E. Greene and J. Singh, "Fabrication of High Thermal Conductivity NARloy-Z-Diamond Composite Combustion Chamber Liner for Advanced Rocket Engines," in *AIAA Science and Technology Forum and Exposition*, San Diego, 2016.

[9] P. Gradl, C. Protz, K. Zagorski, V. Doshi and H. McCallum, "Additive Manufacturing and Hot-fire Testing of Bimetallic GrCop-84 and C-18150 Channel-Cooled Combustion Chambers Using Powder Bed Fusion and Inconel 625 Hybri Directed Energy Deposition," in *55th AIAA/SAE/ASEE Joint Propulsion Conference*, Indianapolis, 2019.

[10] ASTM International., "E8/E8M-16ae1 Standard Test Methods for Tension Testing of Metallic Materials," ASTM International, West Conshohocken, PA, 2016.

[11] P. Gradl, S. E. Greene, C. Protz, B. Bullard, J. Buzzel, C. Garcia, J. Wood, K. Cooper, J. Hulka and R. Osborne, "Additive Manufacturing of Liquid Rocket Engine Combustion Devices: A Summary of Process Developments and Hot-Fire Testing Results," in *54th AIAA/SAE/ASEE Joint Propulsion Conference 2018*, Cincinatti, 2018.

[12] J. Schindelin, C. T. Rueden, M. C. Hiner and K. W. Eliceiri, "The Imagej ecosystem: An open platform for biomedical image analysis," *BMC Bioinformatics,* vol. 82, no. 7-8, pp. 518-529, 2017.